FABRICATION OF TITANIUM DIOXIDE NANORODS ARRAY FOR ULTRAVIOLET SENSOR APPLICATION

SALINA BINTI MOHAMMAD MOKHTAR

UNIVERSITI TUN HUSSEIN ONN MALAYSIA

FABRICATION OF TITANIUM DIOXIDE NANORODS ARRAYS FOR ULTRAVIOLET SENSOR APPLICATION

SALINA BINTI MOHAMMAD MOKHTAR

A thesis submitted in
fulfillment of the requirement for the award of the
Degree of Master in Electrical Engineering

Faculty of Electrical and Electronic Engineering
Universiti Tun Hussein Onn Malaysia

MAY 2017

This thesis was dedicated to my parents; Mohammad Mokhtar bin Mohammad,
Rabiah binti Ibrahim,
and my husband; Mohamad Najib bin Kammalluden

ACKNOWLEDGEMENT

First and foremost, I would like to thank my research supervisor, Assoc. Prof. Dr. Mohd Khairul bin Ahmad for his guidance and encouragement throughout the research. My thesis would not have been possible without his excellent supervision. I would like to express my sincere appreciation to my co-supervisor, Dr. Mohamad Hafiz bin Mamat for his advice and support for this research.

Many thanks to my colleagues in Microelectronic and Nanotechnology Shamsudin Research Centre (MiNT-SRC), particularly Noor Kamalia Abd Hamed, Fatin Izyani Mohd Fazli, Muhammad Luqman Mohd Napi, Asyikin Sasha Mohd Hanif, Nurliyana Mohamad Arifin, Ng Kim Seng, Nur Fakhriah, Sakinah Mohd Khalid, and others, for their help, motivation, kindness, and support during my studies. I also would like to thank Universiti Tun Hussein Onn Malaysia amd Ministry of Higher Education for the scholarship and financial support.

My special thanks to Prof. Masaru Shimomura and Prof. Kenji Murakami from Shizuoka University for their support of this research, including advice and research facilities. I gratefully acknowledge MiNT-SRC staffs, Ms. Isrihetty ans Mrs. Faezahana for their assistance in the lab.

Finally, I would like to express my deepest thanks to my mother, Rabiah Ibrahim and to my husband, Mohamad Najib, mother and father-in-law, Zakiah Ayob and Kammalluden Abd Majid, sisters, Sarah, Syuhada, Nur Farina Emawati, Nurul Nadia, and brothers, Ahmad Muzani, Ahmad Safwan, Wan Rosli, and Mohamad Zairi, for their love, encouragement, understanding, and support during my entire research period.

LIST OF PUBLICATIONS

1. **S. M. Mokhtar**, M. K. Ahmad, N. M. A. N. Ismail, M. S. Mamat, F. I. M. Fazli, N. K. A. Hamed, M. L. M. Napi, N. S. Khalid, N. K. Seng. N. Zainal, S. C. Fhong, N. Nayan, & A. B. Suriani, "Fabrication Of Co/SnO_2 On Glass Substrate Using Spray Pyrolysis Deposition Technique With Variation Of Annealing Temperature", ARPN Journal of Engineering and Applied Sciences (JEAS), vol. 11, no. 14, pp. 8873-8877 (2016).
2. **S. M. Mokhtar**, M. K. Ahmad, N. M. A. N. Ismail, A. B. Suriani, "Fabrication of Titanium Dioxide (TiO_2) Nanorods Array with Various Reaction Times Using One Step Hydrothermal Method", ARPN Journal of Engineering and Applied Sciences (JEAS), (2017), (Submitted)
3. M. K. Ahmad, **S. M. Mokhtar**, C. F. Soon, N. Nafarizal, A. B. Suriani, A. Mohamed, M. H. Mamat, M. F. Malek, M. Shimomura, and K. Murakami, "Raman investigation of rutile-phased TiO2 nanorods/nanoflowers with various reaction times using one step hydrothermal method," J. Mater. Sci. Mater. Electron. (2016).
4. M. L. M. Napi, M. F. Maarof, C. F. Soon, N. Nayan, F. I. M. Fazli, N. K. A.Hamed, **S. M. Mokhtar**, N, K, Seng, M. K. Ahmad, A. B. Suriani, & A. Mohamed, "Fabrication of Fluorine Doped Tin Oxide (FTO) Thin Films Using Spray Pyrolysis Deposition Method For Transparent Conducting Oxide", ARPN Journal of Engineering and Applied Sciences (JEAS), Vol. 11, no. 14, pp. 8800-8804 (2016).
5. F. I. M. Fazli, A. N. Suhaimi, N. S. Khalid, N. K. A. Hamed, M. L. M. Luqman, **S. M. Mokhtar**, N. K. Seng, N. Zainal, N. Nayan, S. C. Fhong, A. B. Suriani & M. K. Ahamd, "The Effects Of Annealing Temperature On Properties Of Aluminium-Doped Tin Oxide (Al/SnO_2) Thin Films Deposited By Spray Pyrolysis Deposition (SPD) Method", ARPN Journal of Engineering and Applied Sciences (JEAS), vol. 11, no. 14, pp. 8840-8845 (2016).

6. N. K. A. Hamed, R. Mahat, N. S. Khalid, F. I. M. Fazli, M. L. M. Napi, **S. M. Mokhtar**, N. K. Seng, S. C. Fhong, N. Nayan, A. B. Suriani, M. K. Ahmad, "Fabrication Of Co/SnO_2 Thin Film for DSSC Using Spray Pyrolysis Deposition Method", ARPN Journal of Engineering and Applied Sciences (JEAS), vol. 11, no. 14, pp. 8873-8877 (2016).

ABSTRACT

Pure rutile titanium dioxide nanorods thin film for ultraviolet sensor application was fabricated on top of bare FTO substrates using hydrothermal method. TiO_2 thin film was developed by optimizing amount of titanium butoxide (TBOT) as a precursor, amount of hydrochloric acid, and hydrothermal reaction time. Basically, there were four properties studied; surface morphology, structural, electrical, and optical properties. Surface morphology of the sample was analyzed by using FESEM. XRD and Raman spectroscopy were used to analyze the structural properties of the thin film. Electrical and optical properties were studied using 2-point probe and UV-vis-NIR spectrophotometer. The first optimization step was to vary the amount of precursor used. Surface morphology of the sample shows that the nanorods growth starts at 3.5 mL of TBOT, and as the precursors increased, diameter and the thickness of the nanorods also increased. Both XRD and Raman show the peaks of FTO and rutile TiO_2. Next, the hydrothermal reaction time was varied. Nanorods diameter and thickness increase with increasing reaction time. XRD and Raman depict FTO and rutile TiO_2 peaks produced. Lastly, the effect of using different amount of hydrochloric acid used was studied. The diameter and thickness of the nanorods decrease as the HCl used increased. Thin film produced was rutile TiO_2 confirmed by both XRD and Raman spectra. The optimized amount of precursor, reaction time, and amount of HCl were obtained at 4.0 mL of TBOT, 16 hour, and 130 mL of HCl, respectively. Study on the optical properties of the TiO_2 thin film shows absorption on ultraviolet wavelength and not on visible wavelength. Electrical analysis shows that the electron flows through TiO_2/FTO interface with conductivity of 0.167 S/m. The thin film was then tested as UV sensor using photoelectrochemical (PEC) method. The rise and decay time recorded was less than then 1 second, indicating a rapid photoresponse characteristics and the photocurrent gives acceptable differences with change in the supplied bias voltage.

ABSTRAK

Filem nipis titanium dioksida (TiO_2) nanorod bagi applikasi pengesan ultraungu telah difabrikasi di atas tin oksida terdop fluorine (FTO) dengan menggunakan kaedah hidroterma. Filem nipis TiO_2 telah dihasilkan dengan menggunakan titanium butoksida (TBOT) sebagai pemangkin, asid hidroklorik, dan air ternyahion. Pada dasarnya, terdapat empat sifat yang dipelajari iaitu permukaan morfologi, struktur, elektrikal, dan optikal. Permukaan morfologi sampel telah dikaji dengan menggunakan FESEM. XRD dan Raman spektroskopi digunakan bagi mengkaji ciri struktur filem nipis. Ciri optikal dan elektrikal dikaji dengan menggunakan *2-point probe* dan *UV-vis-NIR*. Kajian ini telah dijalankan dengan mengoptimumkan masa reaksi, jumlah pemangkin yang digunakan, dan jumlah asid hidroklorik yang digunakan. Proses optimasi yang pertama adalah dengan mempelbagai jumlah pemangkin yang digunakan. Permukaan morfologi menunjukkan bahawa penumbuhan nanorod bermula pada jumlah 3.5 mL TBOT, dan apabila jumlah pemangkin naik, garisan pusat dan ketebalah nanorod turut menaik. Kemudian, masa reaksi hidroterma telah dipelbagaikan. Garisan pusat dan ketebalan nanorod menaik apabila masa hidroterma dinaikkan. Yang terakhir, kesan menggunakan jumlah asid hidroklorik yang berlainan telah dipelajari. Garisan pusat dan ketebalah menurun apabila jumlah asid yang digunakan menaik. Nanorod TiO_2 menunjukkan ciri serapan yang bagus pada gelombang ultraungu. Analsis elektrikal menunjukkan bahawa elektron mengalir diantara permukaan TiO_2/FTO dengan nilai konduksi sebanyak 0.167 S/m. Filem nipis itu kemudian diuji sebagai pengesan ultraungu menggunakan kaedah fotoelektrokimia. Masa menaik dan menurun adalah kurang daripada satu saat, menunjukkan tindak balas foto yang tinggi, dan fotoarus menunjukkan perbezaan yang tidak ketara dengan nilai voltan pincang yang berbeza.

CONTENT

LIST OF FIGURES

LIST OF TABLES

LIST OF SYMBOL AND ABBREVIATIONS

A	-	Cross sectional area
Au	-	Gold
CBD	-	Chemical bath deposition
cm	-	Centimeter
d	-	Diameter
DI	-	Deionized water
DSSC	-	Dye-sensitized solar cell
EMU	-	Electrochemical measuring unit
FE-SEM	-	Field-emission scanning electron microscope
FTO	-	Fluorine-doped tin oxide
GaN	-	Gallium nitiride
HCl	-	Hydrochloric acid
L	-	Length
O_2	-	Oxygen
R	-	Resistance
R_s	-	Sheet resistance
Si	-	Silicon
SiC	-	Silicon carbide
t	-	Thickness
TBOT	-	Titanium butoxide
TiO_2	-	Titanium dioxide
TTIP	-	Titanium isopropoxide
UV	-	Ultraviolet
V	-	Voltage
XRD	-	X-ray diffraction
ZnO	-	Zinc oxide
ρ	-	Resistivity

LIST OF APPENDICES

CHAPTER 1

INTRODUCTION

1.1 Research background

TiO_2 has became known as a potential material to use in UV sensor applications. It can strongly absorb UV light because it has an indirect [1] and wide band-gap energy. Conductivity of TiO_2 rise when UV light is illuminated, making the electrons from valence band excited to the conduction band. A signal produced, due to the excitation that given increase in conductivity, that is used for UV light detection. There are several TiO_2 structures that can be produced such as microspheres, nanoflowers, nanotrees, and nanobelts [2] depending on the technique used. Example of the techniques include chemical bath deposition (CBD), hydrothermal method, sol-gel method, and RF sputtering. However, solution-based techniques are favored in producing high-quality TiO_2 as it is consuming low cost and therefore allowing the fabrication of UV sensors at minimal price. Moreover, by the addition of a stabilizer or surfactant, the growth of TiO_2 structure can be easily controlled. The solution-based can also promotes the growth of TiO_2 at low temperature with large-scale, simple processing methods [3]. Highly crystalline rutile TiO_2 has been intensively investigated due to its advantages such as easily controllable diameter and thickness [4], and higher electron mobility [5,6]. It also has advantages such as higher chemical stability, cheaper production cost [7] and thermodynamically stable [8].

Photo-detection in the ultraviolet (UV) area has attracted attention due to its numerous applications in industry, instrument, and our daily life. Ultraviolet light is defined as a portion of the electromagnetic spectrum that includes visible light, radio waves, X-rays and microwave, with wavelength ranging from 100 to 400 nm that can be further subdivided to: Vacuum UV (100-200 nm), UVC (200-280 nm), UVB (280-315 nm), and UVA (316-400 nm) [9]. It has wavelength that is shorter than visible light, but longer than X-rays as shown in Figure 1.1. Ultraviolet light is used in various applications, including cancer therapy, chemical synthesis, jaundice treatment for new-born babies [10], and drug detection. However, overly exposed to overdose radiations can gives harm to human health. For example, overexposure to UV radiation can causes skin burning and possible skin cancer [11]. Nowadays, research on higher performance UV light sensor are continuously being developed as many situations requiring the monitoring of UV irradiation. Ultraviolet sensor is a device that measures UV light from the sun. it is used in wide range of applications including fire detection, industrial manufacturing, biochemical research, and environmental health monitoring. The traditional electrical UV sensor, which consist of a sensitive photodiode that generates a photocurrent when exposed to UV light, is well established. The current is then converted into a voltage signal and amplified for easier detection. The sensing element of the traditional UV sensor is the photodiode, which is commonly based on silicon.

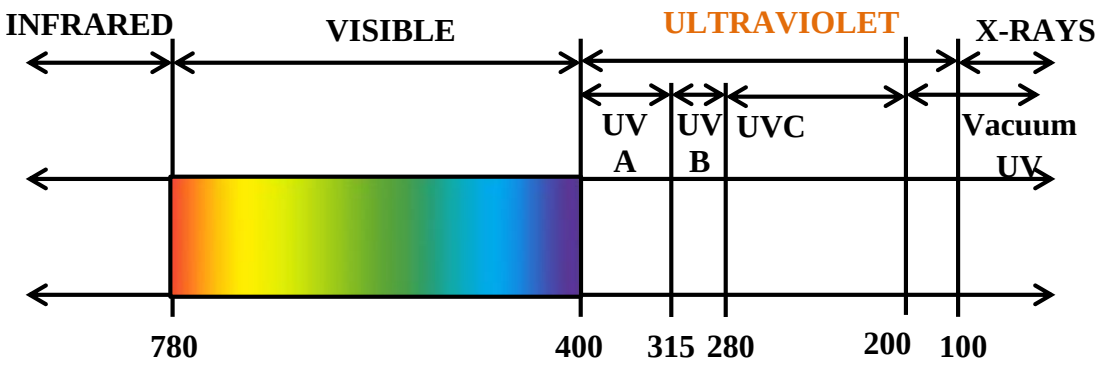

Figure 1.1: Electromagnetic spectrum showing the wavelength of three types of ultraviolet that is UVA, UVB, and UVC

1.2 The properties of titanium dioxide

Titanium dioxide (TiO_2) is a compound that gained much attention for its uses in various applications including photocatalysis [12–14], photovoltaics [15–17], and photosensors [18]. Titanium dioxide, also known as titanium oxide or titania, is found in three natural crystalline phases that is anatase, rutile and brookite, which is thermally and chemically resistant [19], with melting point of 1825°C showing its strong chemical bonding. However, only the first two, which are anatase and rutile, play the role in industrial application because of the rareness and difficult preparation for brookite [20]. TiO_2 has been reported to be an intrinsically, n-type semiconductor due to its oxygen deficiency [21,22]. However, under certain growth condition, it can be found as p-type semi-conductivity behavior [23].

Structure of rutile and anatase are both tetragonal with different space groups. Rutile has space group of $P4_2/mnm$ with two TiO_2 formula units in one cell, while anatase belongs to group $I4/amd$ with four TiO_2 formula units in one cell [24]. The primitive cell unit for rutile is illustrated in Figure 1.2, where the large and small spheres represent the Ti and O atoms respectively. For all three TiO_2 polymorphs, the centre TiO_6 octahedra form their basic structural unit. The difference in these polymorphic structural is the number of edge-shared octahedra, which is two, three and four for rutile, brookite, and anatase, respectively [25]. Figure 1.3 shows the schematic illustration of the formation mechanisms of the anatase and rutile crystal phase [26].

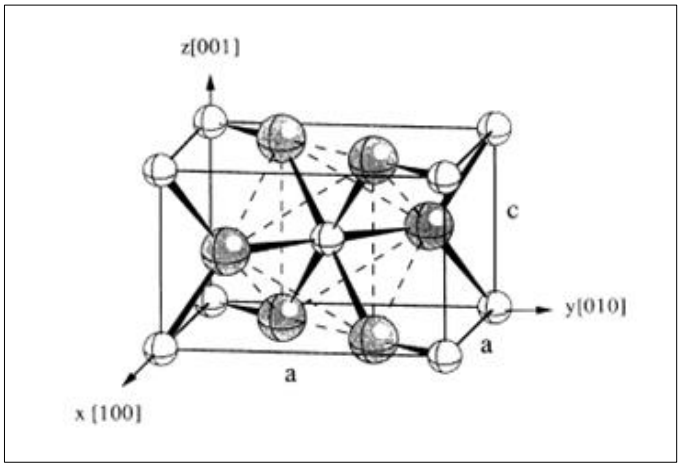

Figure 1.2: The primitive cell unit for rutile TiO_2 [19]

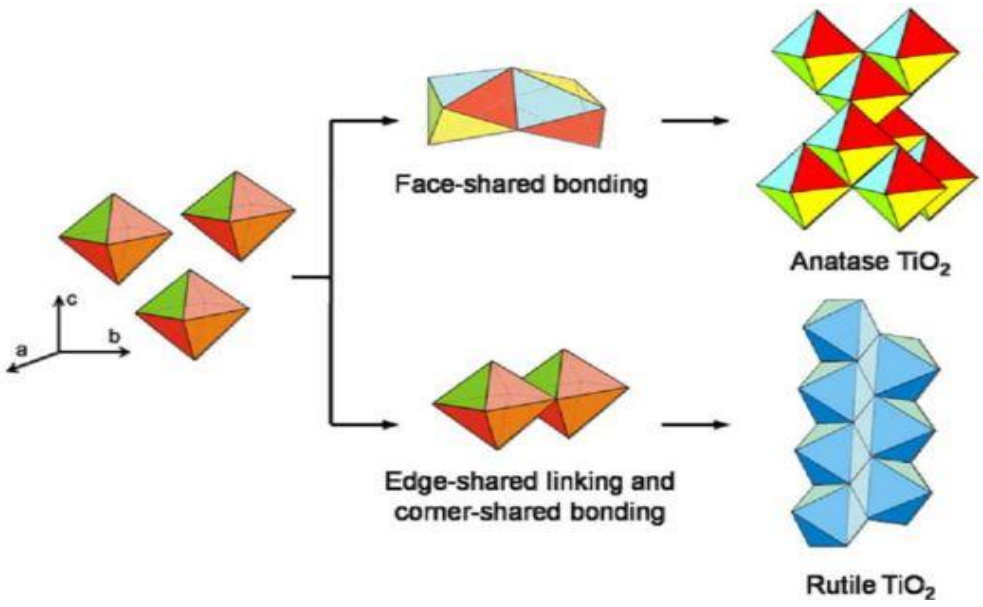

Figure 1.3: Schematic illustration of the formation mechanisms of the anatase and rutile crystal phase [26]

Titanium dioxide is said to be an essential material because of its functional properties. It can absorb UV light and is transparent to visible light spectrum under certain conditions [27]. Additionally, TiO_2 is substantially less expensive than other materials and their reserve is abundant [28]. Its properties can also be altered chemically to enhance its properties, for example, through doping process, which can provide free carriers to increase its efficiency as a photo-catalyst depending on the type of dopants used as different dopant may not have the same effect on trapping electrons and/or hole [29]. It is also non-toxic and chemically inert [30]. The ability of TiO_2 to transmit light spectrum allows for their use in solar cell technology as transparent electrodes [31–33]. In nanomaterials, specific surface area and surface-to-volume ratio would increase as the size of nanomaterials decreases [34]. For TiO_2-based device, the high surface area from small particle size would be advantages. Thus, the performance of TiO_2-based devices was primarily impacted by the sizes of TiO_2 materials itself, particularly at nanometer scale.

1.3 Problem statement

Conventionally, narrow bandgap semiconductors such as silicon is widely used for UV photoconductive sensor applications [35]. However, these Si-based devices also reacted to visible light. Hence, to block the intervention of the visible light, a filters are required to be installed [36]. The necessity of this filter has indirectly increased the production cost. Enquiry on materials with wide band gap such as silicon carbide (SiC), gallium nitride (GaN), and TiO_2 have been made by researchers in order to tackle this problem. The use of filters can be entirely eliminated as these materials have a wide bandgap. Furthermore, devices with these materials give an effective detection of UV light. Additionally, in producing high-quality materials using GaN and SiC, high cost of the equipment and difficult fabrication process is required making it not cost effective. For instance, producing high-quality GaN is possible only if the fabrication process temperature is above 500°C [37].

Additionally, TiO_2 preparation using hydrothermal method is rarely reported for UV sensor application. Hydrothermal method has advantages to easily control the growth of the nanorods. Electrical properties such as low sheet resistance and high conductivity of TiO_2 nanorods thin film will enhance the TiO_2 thin film properties and also improve the efficiency of the sensing devices.

1.4 Research objectives

Because of their distinct properties, titanium dioxide nanorods are now one of the promising nanostructured materials to be applied in UV sensor application. Optimization of fabrication process is essential in order to achieve high performance value of UV-sensing device. For that reason, this work has been carried out with three main objectives that are:

I. To fabricate and optimize TiO_2 nanorods array via hydrothermal method on top of FTO as a substrate
II. To analyze the morphological, structural, optical and electrical properties of aligned TiO_2 nanorods array.
III. To investigate the photocurrent performance, rise time and decay time of aligned TiO_2 nanorods array as ultraviolet sensor.

1.5 Scope of the study

To achieve the objectives, the following scopes were investigated:

i. Several parameters were optimised to get the desired nanorod TiO_2 which are the amount of precursor, hydrothermal reaction time, and amount of the hydrochloric acid.

ii. The fabricated TiO_2 thin film were then analyzed using FESEM, XRD, Raman, 2-point probe, and UV-vis-NIR for its morphological, structural, electrical, and optical properties.

iii. The photocurrent performance, rise and decay time of the optimized nanorod was investigated using photoelectrochemical method for its sensing capabilities.

CHAPTER 2

LITERATURE REVIEW

2.1 Introduction

In this chapter, the history and past research work of hydrothermal and UV sensors were discussed. There are three subtopics that will be discussed including titanium dioxide, hydrothermal, and ultraviolet sensor.

2.2 Titanium dioxide

Titanium dioxide (TiO_2) exists in three known crystalline that is anatase, rutile, and brookite with polymorphs tetragonal for anatase and rutile, and orthorhombic for brookite [38]. TiO_2 have received significant notice these past few decades after the discoveries of photoelectrochemical cell (PEC) and dye sensitized solar cell. The wide range of application, chemical and biological inertness, low cost, eligibility for many experimental techniques and possibility of modifying its properties are the main forces for pursuing research on TiO_2. It is also used in heterogeneous catalysis, as a photocatalyst, a white pigment in all kinds of paints, in paper and cosmetics, antireflection coatings in silicon solar cells and thin films optical devices, as well as an anti-corrosion protective coating [39–42].

Major drawbacks of TiO_2 nanoparticles related to its recombination process during cell performance [43]. To overcome the drawback, TiO_2 nanostructures such as nanorods, nanoflowers, and nanowires, were introduced as its exhibit excellent

electron transport due to its well-defined crystalline structure and unique optical properties, which minimizes the recombination process and have been considered as a substitute in the solar cells and electronic devices.

2.2.1 Titanium dioxide nanorods array

The development of TiO_2 nanostructures in various applications has been progressively conducted [44–47]. Excellent carrier transport properties and large surface area availability makes an array of one-dimensional TiO_2 nanostructures such as nanowires, nanorods, and nanotubes appear to be as potential materials for device fabtrication. Among these structures, nanorod or nanotube has been reported to be better in electron transport and recombination behaviour in liquid based analysis [48].

There have been numerous reports on the fabrication of TiO_2 nanorods array prepared by a variety of techniques. One of the techniques used is 'dissolve and grow' hydrothermal technique, where a rectangular bunched TiO_2 nanorods array was grown on carbon fibres from titanium foil by Wenxi Guo et al [49]. After a corrosion process in a strong acid solution, every single nanorods is etched into a number of small nanowire. The diameter and length of the nanorods were found to be ~150 nm and ~3 μm, respectively.

The work by Zhang H et al has also been referred [50]. They grew a perpendicularly aligned and highly ordered nanorods/nanotubes (NR/NT) adjacent film by directly anodizing a modified titanium foil. The titanium foil substrate was modified with a layer of crystalline TiO_2 film via hydrothermal process in 0.05M $(NH_4)_2S_2O_8$. This resulted to the top layer consisting a highly ordered nanorod connected to array of nanotube at the bottom layer. The thickness of the top nanorod layer was ~90 nm with average nanorod diameter of 22 nm after 20 min of anodization. The thickness of the bottom nanotube layer was found to be 250 nm after 20 min of anodization, with an average outer and inner tubular diameter of 120 and 80 nm, respectively.

Bonil Koo et al. also fabricated TiO_2 nanorods and this time they used non-hydrolytic sol-gel reaction by continuously delivered two titanium precursor using two separate syringe pumps [51]. The length of resulting TiO_2 nanorods increased as

the injection decreased. First reaction was performed with an injection rate of 30 mL/h and the nanorods produced are 6 nm in thickness and 50 nm in length. When the injection rate was decreased to 2.5 mL/h, the nanorods produced are in the dimension of 25 nm to 9 nm in width and 200 to 100 nm in length. Nanorods with dimensions of 25 nm x 450 nm were synthesized when the injection rate was further decreased to 1.25 mL/h. In this experiment, the simultenous phase transformation and length elongations of the TiO_2 nanorods were achieved.

Another method to grow TiO_2 nanorods was by using sol electrophoretic deposition that is done by Limmer et al [52]. They produced nanorods with a diameter size ranging from 45 – 200 nm in diameter and 10 – 60 μm in length after annealed it to 500 °C for 1 hour in a template membrane of polycarbonate and alumina with aluminium (Al) and Indium Tin Oxide (ITO) as a glass template, respectively. Their study shows that the growth occurs through the motion of charged nanoparticles from the bottom of the template pores, filling them up as time proceeds.

K. Fujihara et al fabricated nanorods by mechanically grinding the TiO_2 nanofibres in which the nanofibres was fabricated by combining sol-gel and electrospinning technique [53]. The average diameter of the composite nanofibers was 290 ± 90 nm which was decreased to 150±60 nm after sintering process to nanorod. Figure 2.1 shows FESEM image of TiO_2 nanorods fabricated by sol-electroporetic and sol-gel electrospinning methods. A comparison of the method used to grow TiO_2 nanorods is summarised in Table 2.1.

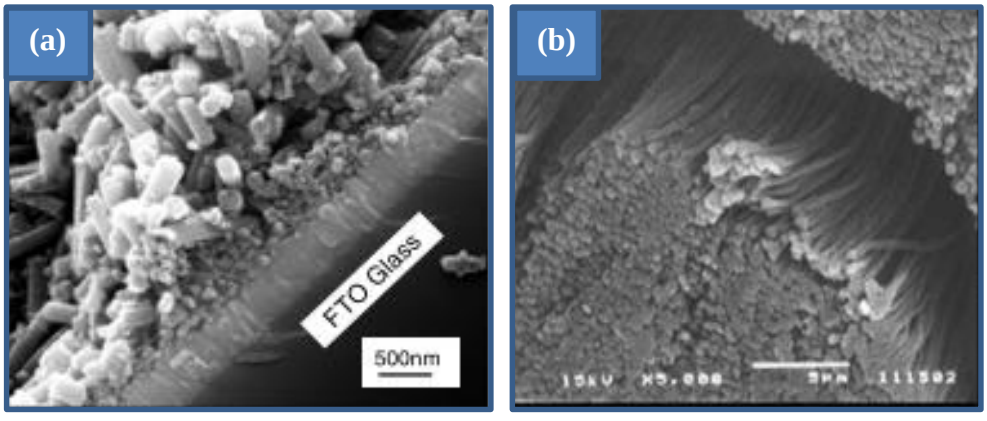

Figure 2.1: TiO_2 nanorods fabricated by (a) sol electrophoretic [52] and (b) sol-gel electrospinning methods [53]

Table 2.1: Comparison of the method used to grow TiO_2 nanorods

Fabrication Method	**Special Features**	**Structure (diameter (d)/length (l)/ thickness (t) if notified)**	**Reference**
Hydrothermal method	Dissolve and grow i. Hydrothermal of NR on carbon fibre (CF) using Ti foil ii. CF ultrasonically cleaned iii. Hydrothermal again for etching process iv. immersed in $TiCl_4$ sol v. Annealed to increase crystallinity	d: 150 nm / l: 3 μm	[49]
Anodizing method	Modified Ti foil using hydrothermal methods i. To obtain crystalline TiO_2 film ii. NR growth not highly ordered	d: 22 nm / l: 90 nm	[50]
Non-hydrolytic sol-gel reaction	Length of NR can be controlled by controlling injection rate i. 30 mL/h ii. 2.5 mL/h iii. 1.25 mL/h	i. 30 mL/h (d: 6 nm, l: 50 nm) ii. 2.5 mL/h (d: 9 nm, l: 100 nm) iii. 1.25 mL/h (d: 25 nm , l: 450 nm)	[51]
Sol electrophoretic deposition	Combination of sol-gel and electrophoretic deposition	d: 45 – 200 nm l: 10 – 60 μm	[52]
Sol-gel and electrospinning	Mechanical grinding of TiO_2 nanofibres to nanorod	d: 150±60 nm	[53]

2.3 Hydrothermal

There are many methods to produce nanostructured material or particles such as DC sputtering, pulse-laser deposition (PLD), and spray pyrolysis method. However, in this thesis, hydrothermal method will be used. Hydrothermal method is a non-

traditional way to obtain nanocrystalline inorganic material. In a self-explanatory word, “hydro” means water, and “thermal” means heat. According to Laudise, hydrothermal growth means growth from aqueous solution at ambient or non-ambient solution. Rabenau defined hydrothermal synthesis as the heterogeneous reactions in aqueous media above 100°C and 1 bar. Roy declares that hydrothermal synthesis involves water as a catalyst and occasionally as a component of solid phases in the synthesis at elevated temperature (>100°C) and pressure greater that a few atmospheres. Byrappa defines hydrothermal synthesis as any heterogeneous reaction in an aqueous media carried out above room temperature at a pressure greater than 1 atm. Yoshimura proposed the following definitions: reactions occurring under the conditions of high-temperature-high-pressure (>100°C, >1 atm) in aqueous in a closed system [30].

From all researchers mentioned above, it shows that hydrothermal method is one of the best methods for material synthesis at low temperature with high pressure in a closed system. By adjusting reactions conditions, many forms of ceramic materials can be synthesized such as fibre, powder, single crystals, nanoparticles, and thin films. This method also allows regulation of rate and uniformity of the nucleation, growth and aging process, which leads to improved size and morphology control.

2.3.1 History of hydrothermal

The term hydrothermal is solely geological origin. It is first described as the action of water at elevate temperature and pressure leading to emergence of different rocks and minerals in the earth crust by Sir Roderick Murchison [54]. Table 2.2 shows the decade-wise evolution of the hydrothermal with regards to its objective and apparatus used [30].

Table 2.2: Evolution of hydrothermal technology with time

Period	Focus	Equipment	Remark
1850-1900	Mineral synthesis, imitation of natural conditions	Simple reactors, glass reactors, digestors	Lower growth rate, tiny particles, geological interest
1900-1940	Mineral synthesis, improvement in PT conditions, German domination	Morey autoclaves, flat closure	Lower growth rate, silicates, carbonates, Germany, Russia, France, USA, geological interest
1940-1950	Large size and large scale production of quartz, beginning of zeolites, clays, and micas	Test-tube type (cold-cone-sealed), welded closure, modified Bridgman type	Cold-cone-seal type autoclaves made revolution, PVT diagrams systems
1950-1960	Phase diagrams for natural systems	Morey, Turtle-Roy, welded closures, modified Bridgman	The dawn of modern hydrothermal research
1960-1970	Synthesis of technological materials, new inorganic compounds without natural analogues	New designs from USSR, commercialization of the autoclaves, improved sealing, larger size of the autoclaves	Russian School dominated, Japanese labs appeared
1970-1980	A variety of new materials synthesis, ceramic processing in a bigger way, advanced materials	New designs, improved PT conditions, Grey-Loc sealing, large autoclaves	Appearance of many hydrothermal labs in several countries
1980-1990	Decline in interest on hydrothermal research. Importance of the technique in materials science, physical chemistry of hydrothermal solutions	-	Japan organized 1st Int, Conf. Hydrothermal Reactions. Beginning of the entry of physical chemist
>1990	Diversification of hydrothermal technique, age of solvo-thermal, physical chemistry of hydrothermal solutions.	Design of new reactors to suit the specific applications: batch reactors, flow reactors, and so on	Entry of organic chemist, environmental scientist, fall in Russian domination and beginning of the Japanese domination

Hydrothermal synthesis is a non-conventional method of synthesizing nanocrystalline inorganic materials. The synthesis method use solubility in water of almost all inorganic substances at elevated temperature and pressure, performed in an apparatus consisting of a steel pressure vessel called an autoclave. These autoclaves are usually thick-walled steel cylinders with a tight seal which ought to withstand high temperature and pressure for prolonged times span. Furthermore, the autoclave material must be inert with the respect to the solvent. The autoclave closure is the most important element. Many designs have been progressed for seals, which the most famous being the Bridgman seal. To prevent corrosion of the internal cavity the autoclave, preservative inserts are generally used. Insert may be made of carbon-free iron, silver, gold, platinum, glass, or Teflon. In this research, the insert used is Teflon. Hydrothermal method is widely used for the production of small particles in the ceramics industry.

2.3.2 Fabrication of TiO_2 nanorods array using hydrothermal method

Nanostructured TiO_2 was synthesized by using hydrothermal processing of titanium alkoxides, such as Titanium Isopropoxide (TTIP) and Titanium Butoxide (TBOT). It has been widely studied and investigated as a photocatalyst and in dye-sensitize solar cell (DSSC). The morphology of the nanorods can be easily adjusted with different surfactants [55] or by changing the solvent compositions [56]. The hydrothermal method is widely used due to its simple processing, fast reaction velocity, and low cost [57]. At relatively lower temperature (~150°) a high degree of crystallinity thin film can be obtained; it also offers a uniform composition, and control over the shape and the size of particles. The hydrolysis reaction between H_2O and TBOT are schematically given as [58]:

$$Ti(C_4H_9O)_4 + 4H_2O \rightarrow Ti(OH)_4 + 4C_4H_9OH \qquad (2.1)$$

Ti from the hydrolysis will then be used as a starting material for nucleation of TiO_2 nanorods. The hydrolysis reaction of hydrothermal process can be explained as follows [49]:

$$2Ti + 6HCl \rightarrow [Ti^{3+}] + 3H_2(g) \quad (2.3)$$

$$[Ti^{3+}] + H_2O \rightarrow TiOH^{2+} + H^+ \quad (2.4)$$

$$TiOH^{2+} + O_2^- \rightarrow Ti(IV) + O_2^- \rightarrow TiO_2 \quad (2.5)$$

Ti species from TBOT precursor initially starts to react with H^+ ions from concentrated acidic solution. It is known that Ti^{3+} are not stable in aqueous solution, thus it undergoes hydrolysis with H_2O to form $TiOH^{2+}$. It is then oxidized to Ti (IV) by reaction with dissolved oxygen. The Ti (IV) complex ions are thus used as the growth unit. The by-product from the reaction does not influence the sample as the sample was first rinsed with DI water before used.

Yawen Wang et al. reported that the synthesis of pure rutile nanorods is by hydrolysis of $TiCl_4$ ethanolic solution in water at 50°C [59]. By simply changing the molar ratio of $TiCl_4$, ethanol or DI water, the assembly of rutile nanorods can be changed to flower and urchin-like morphologies. By playing around with the amount of ethanol and $TiCl_4$ used, the resulting rods seems becoming more complex with increasing amount of the solution. They also studied the effect of H^+, Cl^-, and ethanol on the morphologies by replacing $TiCl_4$ with TTIP and adding some additives such as KCl, HNO_3, and H_2SO_4. It can be concluded that the strong acidic condition from H^+ and Cl^- was crucial for the formation of rutile TiO_2 and ethanol is needed for the formation of rutile TiO_2 in the absence of seed nanocrystal or organic surfactant additives. Nanorods produced were of 10-15 nm in diameter and 50-70 nm in length. Doubling both amount $TiCl_4$ and ethanol gives diameter of the nanorods 4-7 nm while the length increased to 80-100 nm. When only the amount of $TiCl_4$ increase, the nanorods agglomerates to well-defined spheres with 200-600 nm in sizes.

Muhammad N. Tahir et al reported on the synthesis of in situ surface-functionalized, monocrystalline rutile TiO_2 nanorods using a hydrothermal method [60]. The rutile TiO_2 nanorods were prepared from $TiCl_4$ in aqueous solution under acidic conditions in the presence of dopamine and are in this study, they use 3-hydroxytyramine. With this amine group functionality on its surface, it offers an excellent prospect for TiO_2 nanobiocomposites and biotracers.

Large-scale, well aligned single crystalline TiO_2 on pre-treated glass substrate by hydrothermal method was prepared by Yuxiang Li et al [61]. The results demonstrated that the TiO_2 was well-aligned and grown along [001] direction with diameter and length of 15 to 25 nm and 300 to 500 nm respectively. The pre-

treatment of the substrate is done by coating the colloidal solution prepared onto the clean glass substrate. It has been shown that the nanorods grown on coated glass substrate has better growth orientation and uniform density.

Another hydrothermal synthesis is done by Yuan et al. on boron-doped diamond film with zinc oxide (ZnO) buffer layer [57]. It is shown that the ZnO buffer layer plays an important role in increasing the density and improving the morphologies of the TiO_2 nanorods. The ZnO buffer layer was so thin that it was not detected on XRD and some of the ZnO nanoparticles may be removed in the hydrothermal process.

Lingqing Dong et al. fabricated rutile TiO_2 nanorods film on titanium substrate via a hydrothermal method [62]. They used Tetra-n-butyl titanate as the source of Ti in the presence of hydrochloric acid. The Ti substrate did not only act as a substrate but also as the source of TiO_2. The nanorods thin film automatically formed even in the absence of a precursor when the rhickness of the TiO_2 reached certain level. They also studied on the influence of metal chlorides on TiO_2 nanorods growth where chlorides such as LiCl, NaCl, and KCl were added into the mother solution. These chlorides affect the diameter and density of the nanorods by decreasing it when LiCl is added and increasing it in the presence of KCl and NaCl.

Hong En-Wang et al. used the hydrothermal method to prepare single-crystalline TiO_2 nanorods [63]. The average diameter and length of nanorods prepared are 60 nm and 400 nm respectively. They stated that this method shows great versatility and can be used to grow TiO_2 nanorods on large diversity of substrate including Si, Si/SnO_2, sapphire, and fluorine-doped tin oxide (FTO).

S. Venkatachalam et al. also used hydrothermal treatment to produce TiO_2 nanowires, nanorods, and nanoporous film [64]. By varying the amount of hydrochloric acid used and the annealing temperature, it is reported that nanorod size increased as the volume of HCl and the temperature in the reaction solution was increased. The nanorods produced have a range of 125 to 310 nm for diameter and 480 nm to 2.6 μm for length when the temperature was increased from 120°C to 160°C. Meanwhile, the nanorod size is in the range of ~150 nm to 200 nm when the HCl increased from 15 to 23 mL and DI water decreased from 45 to 30 mL. These studies shows that, solution-based synthesis generally, and hyrothermal fabrication method specifically, gives promising results in producing TiO_2 nanorods array. A

comparison of hydrothermal technique used to fabricate TiO_2 nanorods array is summarised in Table 2.3.

Table 2.3: Comparison of hydrothermal technique used to fabricate TiO_2 nanorods array

Additional features	**Diameter (d) and Length (l)**	**Reference**
Changing the molar ratio of $TiCl_4$, ethanol or DI water	d: 10 – 15 nm l: 50 – 70 nm	[59]
NR was prepared from $TiCl_4$ under acidic conditions + dopamine	d: 15 – 16 nm l: 40 – 100 nm	[60]
Pre-treated glass substrate; coating colloidal solution	d: 15 – 25 nm l: 300 -500 nm	[61]
Using boron-doped diamond film with ZnO as a buffer layer	d: 50 – 80 nm l: 280 nm	[57]
Used Ti as a substrate where it also acts as a source of TiO_2. Study the effect of chlorides to NR growth	d: 10 – 20 nm l: 800 – 900 nm NR diameter increased with KCl and NaCl, decreased with LiCl	[62]
Using different types of substrate: Si wafers, Si/SiO2 wafer, sapphire, Si pillars, and FTO-covered glass	d: 60 nm l: 400 nm	[63]
Varying amount of hydrochloric acid	d: 150 – 200 nm l: 480 nm – 2.6 µm	[64]

2.4 Ultraviolet Sensor

Flame detections, space communications, ozone layer monitoring, and UV astronomy are among the technology that are using UV photoconductive sensor [65]. Nowadays, fabrication of UV photosensor are gaining attention due to its applications in different fields. Among the materials that are being utilised in fabricating UV sensor is silicon (Si), gallium nitride (GaN), zinc selenide (ZnSe), Silicon carbide (SiC) and diamond [65–68]. Using Si materials as a UV sensor have

caused several problems. First, Si has a low bandgap, which is 1.1eV; causing low responsivity towards ultraviolet radiation and requiring a visible light filter if applied in the device structure [69]. Si is also not suitable to be used as it has limitation in harsh environmental conditions, for example UV detection at high temperature [70]. Meanwhile, GaN, SiC, and diamond shows a decent performance under high temperature conditions. However, the materials are not cost effective as they have high fabrication cost making it not fitting for large scale production [71].

2.4.1 Ultraviolet sensor using titanium dioxide nanomaterials

A number of materials, including TiO_2 nanostuructured have been proposed and studied intensively in order to fabricate a UV sensor with good stability and reliability at a reasonable prices. Among the TiO_2 nanomaterials that have been used for UV detectors are TiO_2 nanoflowers. For an example of fabrication of TiO_2 nanoflowers UV photoconductive sensors, the work by Xihong Zu et al. has been referred [72]. By using combined method of hydrothermal and in-situ multiple wet chemical depositions method, the successfully constructed structure was composed of heterostructured arrays of TiO_2 nanowires (NWs) and polyaniline nanoflowers (PANI NFs) in sandwiches form. With comparison to 254 nm, the resulting photodetector exhibits excellent UV sensitivity and fast response speed with UV illumination at 365 nm wavelength.

Another work by Huan Wang et al. also used the same structure of sandwiches layer of TiO_2 and PANI [73]. But this time, the TiO_2 are nanorods (TNRs) structure and the PANI layer are nanowires (PANI NWs). The fabrication method used for PANI NWs was the chemical oxidation method meanwhile TNRs are synthesized using hydrothermal method. This work has also been tested using two UV wavelengths that are 254 and 365 nm. The 365 nm UV photocurrent of the designed UV photodetector was as high as 3.5×10^{-4} A, and 254 nm UV photocurrent was only 0.16×10^{-4} A. This study can provide opportunities for developing devices that can recognize different wavelengths of UV light.

W. F. Xiang et al. fabricated two types of nanocrystalline TiO_2 films; porous (P-detector) and dense (D-detector), on FTO substrates by two step approaches that are hydrothermal and the adding of polyethylene glycol to form nanocrystalline TiO_2

solution [74]. They used two colloidal silver electrodes as top electrode for TiO_2 surface and bottom electrodes for FTO separated by about 3 mm. The rise time and decay time of the P-detector and D-detector are 19 and 136 ns, and 14 and 100 ns, respectively. By comparing these two types of detector, P-detector is found to give higher responsivity due to a light scattering effect.

Another solution-based technique that is spray pyrolysis deposition (SPD) is used by Masayuki Okuya et al for UV sensor application [75]. The measurement was carried out under the light intensity of 20 $\mu W/cm^2$ irradiated directly on the sensors. The fabrication process varied the solvent used among ethanol, 2-propanol, and 2-butanol in which the results showed that ethanol gives the higher intensity from photo response of UV sensors. The UV response of the photodiode became more sensitive with increasing porosity of TiO_2 layer deposited from ethanol solution. Sensitivity of the UV sensor can be improved in this study by doping a little amount of aluminium to reduce the depletion layer. The photo response of TiO_2 UV sensor fabricated with aluminium layer showed higher intensity than that fabricated without aluminium layer.

An ultraviolet sensor based on TiO_2 nanorods that are grown on a p-type substrate seeded with a TiO_2 layer and synthesized by radio frequency reactive magnetron sputtering was done by Abbas M. Selman et al [76]. The TiO_2 nanorods were grown by using chemical bath deposition (CBD) method. The device showed 3.79×10^2 sensitivity when it was exposed to 325 nm light at 5V bias voltage.

2.4.2 Ultraviolet sensor mechanism

The enhancement of TiO_2 conductivity during dark and UV illumination can be explained as follows [77]. Both intrinsic conductivity and the conductivity of TiO_2 in the dark can be described by equation 2.4:

$$\sigma = en\mu \qquad (2.4)$$

Where σ is the conductivity, *e* is the electronic charge, *n* is the charge carrier density, and μ is the carrier mobility. Under a bias voltage across the metal contact gap, the current density, *J*, can be found by equation 2.5:

$$J = \sigma F \text{ where } F = V / \text{x} \qquad (2.5)$$

Here, *F* is the applied electric field, *V* is the bias voltage, and x is the distance. Under UV illumination, a change in photoconductivity, $\Delta\sigma$, occurs either by a change in the carrier concentration, Δn, or by a change in the carrier mobility, $\Delta\mu$, as indicated by the equation 2.6:

$$\Delta\sigma = \sigma_{\text{light}} - \sigma_{\text{dark}} = e\,(\mu\Delta n + n\Delta\mu) \qquad (2.6)$$

Generally, the photocurrent density, $J_{photocurrent}$, can be expressed as a function of time by equation 2.7:

$$J_{photocurrent} = [\mu(t)\Delta n(t) + \text{n}(t)\Delta\mu(t)]\, eF \qquad (2.7)$$

In many semiconductors, the change in mobility can be entirely neglected because $\Delta n >> \Delta\mu$; therefore, the equation can be simplified as equation 2.8:

$$\begin{aligned} J_{photocurrent} &= \Delta\sigma F \\ &= e\mu\Delta n(t)F \end{aligned} \qquad (2.8)$$

From this equation, it can be concluded that the photoconductivity of TiO_2 UV sensor depends on the mobility, carrier concentration, and the electric field or the bias voltage. Thus, to increase the photocurrent of the device, these three parameters must be improved. For example, the mobility of TiO_2 can be enhanced by using highly crystalline TiO_2 nanostructures such as nanowires or nanorods. Additionally, the carrier concentration of TiO_2 can be increased by the doping process.

According to the previous study, the photoconduction of UV sensor is governed by oxygen adsorption and desorption on its surface, as shown in Figure 2.2 [78]. This mechanism is widely accepted as the cause of high photocurrent values under UV illumination as the lifetime of the photoexcited electron is increased. According to this mechanism, surrounding oxygen molecules can be adsorbed onto the nanorods surface by capturing the free electrons from the TiO_2 nanostructure, as shown in 2.9:

$$O_2 + e^- \rightarrow O_2^- \qquad (2.9)$$

Where O_2 is the oxygen molecule, e^- is a free electron, and O_2^- is adsorbed oxygen on the nanorod surface. This process is illustrated by Process 1 in Figure 2.2. The adsorption of oxygen onto the surface causes bend bending. When UV light is incident on the surface of the nanostructure, electron-hole pairs are generated according to the following equation 2.10:

$$h\nu \rightarrow h^+ + e^- \qquad (2.10)$$

Where $h\nu$ is the photon energy from the UV light, h is a plank's constant, v is the photon frequency, h^+ is a photogenerated hole in the valence band, and e^- is the photogenerated electron in the conduction band. Large surface area is needed as it facilitates fast surface reaction as the photogenerated hole reacts with negatively charged adsorbed oxygen, as shown by equation 2.11:

$$O_2^- + h^+ \rightarrow O_2 \qquad (2.11)$$

This process releases oxygen molecules from the nanorods surface as shown by Process 2 in Figure 2.2. This will cause hole trapping phenomenon at the TiO_2 surface, as illustrated by Process 3 and Process 4, and leaves behind the electron of the pair, as indicated by Process 5 and Process 6, which results in increasing of the conductivity of the nanostructures. The unpaired e^- will either collected at the metal contact or recombine with the holes when the oxygen is re-adsorbed on the TiO_2 surfaces, as shown by Process 7 in Figure 2.2. The maximum photocurrent can be achieved when the generation rate of the electron-hole pairs and recombination is equivalent. When illumination is removed, the oxygen molecule recombines with the electron, leading to the decrease in film conductivity.

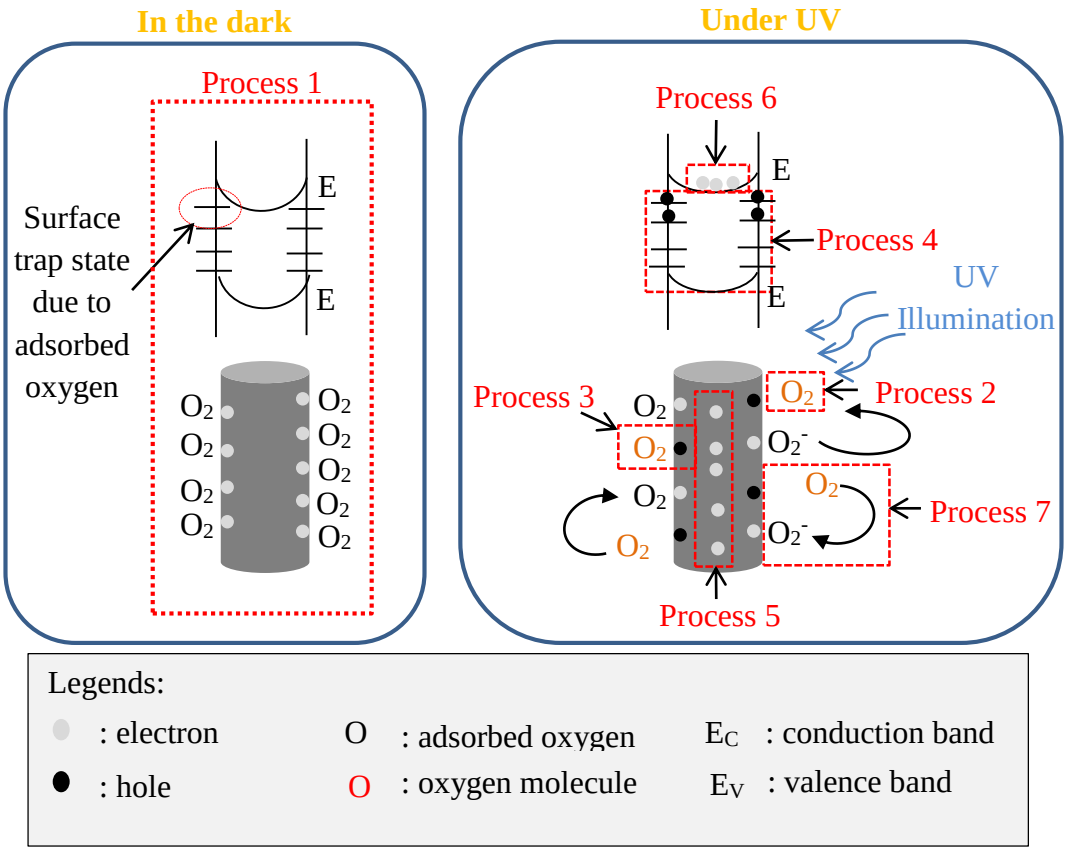

Figure 2.2: The mechanism of photoconduction in TiO_2-based UV sensor under dark and UV illumination conditions

CHAPTER 3

METHODOLOGY

3.1 Introduction

In this chapter, preparation of the titanium dioxide (TiO_2) nanorods using hydrothermal synthesis is presented. Three main topics will be explained in this chapter including substrate cleaning, preparation of the TiO_2 solutions for nanorods array using hydrothermal methods, and the characterisation methods including surface morphology study, chemical composition, electrical, and optical properties. The experimental details are given in the subsequent chapter. Figure 3.1 shows the flow chart for nanostructured TiO_2 thin film preparation and characterization.

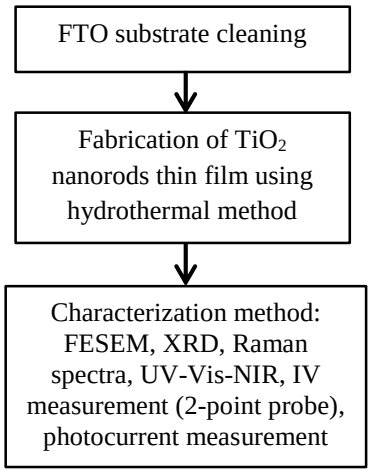

Figure 3.1: Summarized of nanostructured TiO_2 thin film preparation and characterization

3.2 Substrate cleaning by sonicating method

Before the fabrications, substrate used, that is fluorine-doped tin oxide (FTO) was cleaned in order to remove contaminants. The contaminations on the FTO might affect the material growth, thus affecting the properties of the material. FTO substrate is a substrate that is transparent, low cost, has high-temperature resistant, and chemically inert. Also, FTO substrate exhibit electrical conductivity and at the same time allows transmission of solar cell radiation on its active region[79]. The substrate cleaning procedure is summarized in Figure 3.2.

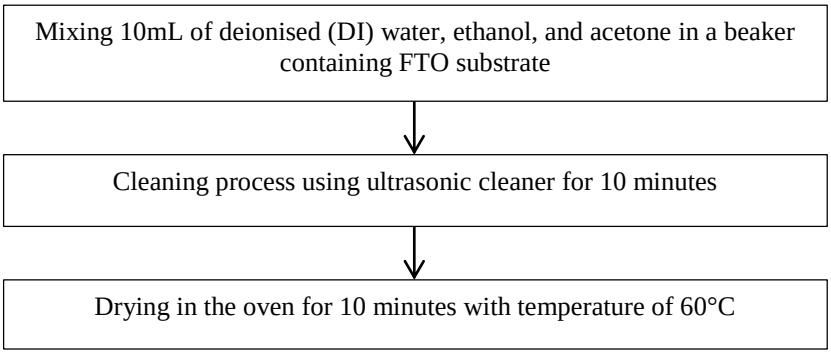

Figure 3.2: Summarized of cleaning substrate procedure

3.3 Preparation of TiO_2 solution for hydrothermal reaction

The TiO_2 hydrothermal were prepared by using titanium butoxide (TBOT) as a precursor (starting material), hydrochloric acid (HCl) as a chelating agent, and deionised water (DI) as a solvent. Chelating agent is ligand that can form bonds (covalent bondings) at more than one point. It is a substances whose molecules can form a several bonds to a single metal ion. Meanwhile, deionised water acts as a function of adding the oxygen (O_2) element into TBOT for hydrolysis process. 120 mL of concentrated hydrochloric acid (HCl) (36.5 % ~ 38 %) was dissolved in 120 mL of DI water as chemical solution for hydrothermal process. The mixture was vigorously stirred for 5 minutes on the hot plate stirrer and then TBOT was added drop wise using a capillary tube. After stirring for nearly 15 minutes, the solution was put into steel made autoclave with Teflon made liner (300 mL) for hydrothermal process in which the FTO glass substrate were put with the conducting FTO surface

facing the walls of the Teflon. Nucleation of TiO_2 seed in the solution leads to the growth of nanoflowers [80,81]. The conductive side of the FTO was put facing the wall to avoid deposition of nanoflowers on top of the nanorods. The autoclave steel used was shown in Figure 3.3. The process was performed at 150°C with a variation of reaction time, volume of TBOT, and volume of hydrochloric acid used. After that, the autoclave was taken out from oven and cooled down in room temperature for 5 hours to allow the steel made autoclave to cool and touchable. The prepared samples were rinsed with DI water and left to dry at room temperature. Figure 3.4 shows the FTO substrate before and after the hydothermal reaction. Summarised step for preparing the solution is shown in Figure 3.5 and the details experimental parameters are tabulated in Table 3.1.

Table 3.1: Preparation of TiO_2 solution for hydrothermal reaction

Solution preparation	**Materials**	**Precursor**	Titanium butoxide
		Chelating agent	Hydrochloric acid
		Solvent	DI water
		Solution volume	240 mL
Fabrication Process	**Hydrothermal**	**Temperature**	150 °C

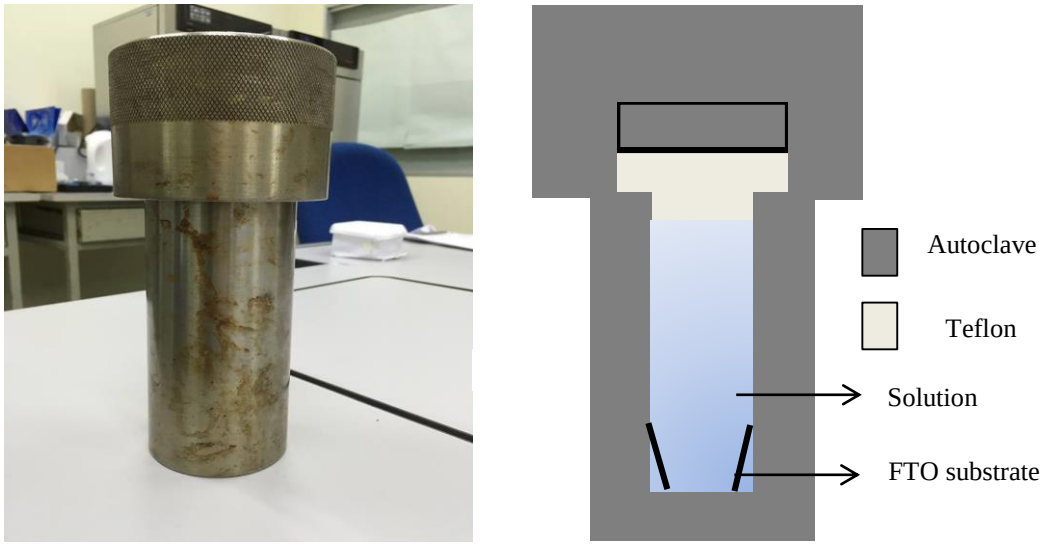

Figure 3.3: Autoclave used for hydrothermal process

REFERENCE

[1] M. C. Mathpal, A. K. Tripathi, M. K. Singh, S. P. Gairola, S. N. Pandey, and A. Agarwal, "Effect of annealing temperature on Raman spectra of TiO_2 nanoparticles," *Chem. Phys. Lett.*, vol. 555, pp. 182–186, 2013.

[2] W. Zhou, X. Liu, J. Cui, D. Liu, J. Li, H. Jiang, J. Wang, and H. Liu, "Control synthesis of rutile TiO2 microspheres, nanoflowers, nanotrees and nanobelts via acid-hydrothermal method and their optical properties," *CrystEngComm*, vol. 13, no. 14, pp. 4557–4565, 2011.

[3] A. C. Arias, J. D. MacKenzie, I. McCulloch, J. Rivnay, and A. Salleo, "Materials and applications for large area electronics: Solution-based approaches," *Chem. Rev.*, vol. 110, no. 1, pp. 3–24, 2010.

[4] Y. Liao, W. Que, Q. Jia, Y. He, J. Zhang, and P. Zhong, "Controllable synthesis of brookite/anatase/rutile TiO_2 nanocomposites and single-crystalline rutile nanorods array," *J. Mater. Chem.*, vol. 22, no. 16, pp. 7937–7944, 2012.

[5] X. Feng, K. Shankar, O. K. Varghese, M. Paulose, T. J. Latempa, and C. a Grimes, "Vertically aligned single crystal TiO_2 nanowire arrays grown directly on transparent conducting oxide coated glass: synthesis details and applications.," *Nano Lett.*, vol. 8, no. 11, pp. 3781–3786, 2008.

[6] E. Hendry, M. Koeberg, B. O'Regan, and M. Bonn, "Local Field Effects on Electron Transport in Nanostructured TiO_2 Revealed by Terahertz Spectroscopy," *Nano Lett.*, vol. 6, no. 4, pp. 755–759, 2006.

[7] E. Hosono, S. Fujihara, K. Kakiuchi, and H. Imai, "Growth of Submicrometer-Scale Rectangular Parallelepiped Rutile TiO_2 Films in Aqueous $TiCl_3$ Solutions under Hydrothermal Conditions," *J. Am. Chem. Soc.*, vol. 126, no. 25, pp. 7790–7791, 2004.

[8] M. Kosmulski, "The significance of the difference in the point of zero charge between rutile and anatase," *Adv. Colloid Interface Sci.*, vol. 99, no. 3, pp. 255–264, 2002.

[9] T. Koutchma, "Basic Principles of UV Light Generation," in *Food Plant Safety*, First., Elsevier, 2014, pp. 3–13.

[10] T. Koutchma, "UV Safety," in *Preservation and Shelf Life Extension*, First., Elsevier, 2014, p. 59.

[11] T. Koutchma, "Fundamentals of UV Light Emission, Transmission, and Absorption," *Preserv. Shelf Life Ext.*, pp. 1–3, 2014.

[12] S. Buzby, M. a. Barakat, H. Lin, C. Ni, S. a. Rykov, J. G. Chen, and S. Ismat Shah, "Visible light photocatalysis with nitrogen-doped titanium dioxide nanoparticles prepared by plasma assisted chemical vapor deposition," *J. Vac. Sci. Technol. B Microelectron. Nanom. Struct.*, vol. 24, no. 3, pp. 1210–1214,

2006.

[13] O. Ola and M. M. Maroto-Valer, “Review of material design and reactor engineering on TiO_2 photocatalysis for CO2 reduction,” *J. Photochem. Photobiol. C Photochem. Rev.*, vol. 24, pp. 16–42, Sep. 2015.

[14] R. Edy, Y. Zhao, G. S. Huang, J. J. Shi, J. Zhang, A. A. Solovev, and Y. Mei, “TiO_2 nanosheets synthesized by atomic layer deposition for photocatalysis,” *Prog. Nat. Sci. Mater. Int.*, vol. 26, no. 5, pp. 493–497, Oct. 2016.

[15] J. Xiong, B. Yang, J. Yuan, L. Fan, X. Hu, H. Xie, L. Lyu, R. Cui, Y. Zou, C. Zhou, D. Niu, Y. Gao, and J. Yang, “Efficient organic photovoltaics using solution-processed, annealing-free TiO_2 nanocrystalline particles as an interface modification layer,” *Org. Electron.*, vol. 17, pp. 253–261, 2015.

[16] P. H. Falla, M. O. G. Dias, H. Vieira, R. da S. P. Junior, L. H. X. da Silva, and P. H. O. Nogueira, “Optimization the Efficiency Photovoltaic Solar Cells Using Synthesized TiO_2 Semiconductor Nanomaterials and Functionalized Carbon Nanotubes.,” *Energy Procedia*, vol. 57, pp. 1860–1867, 2014.

[17] Y.-M. Sung, “Deposition of TiO_2 Blocking Layers of Photovoltaic Cell Using RF Magnetron Sputtering Technology,” *Energy Procedia*, vol. 34, pp. 582–588, 2013.

[18] M. Okuya, “Porous TiO_2 thin films prepared by spray pyrolysis deposition (SPD) technique and their application to UV sensors,” *Solid State Ionics*, vol. 172, no. 1–4, pp. 527–531, Aug. 2004.

[19] E. N. Bunting, “Phase equilibria in the systems TiO_2, TiO_2-SiO_2 and TiO_2-Al_2O_3,” *Bur. Stand. J. Res.*, vol. 11, no. November, 1933.

[20] M. Landmann, E. Rauls, and W. G. Schmidt, “The electronic structure and optical response of rutile, anatase and brookite TiO_2.,” *J. Phys. Condens. Matter*, vol. 24, no. 19, p. 195503, 2012.

[21] L. Forro, D. Emin, L. Zuppiroli, D. De Physique, E. Polytechnique, F. De Lausanne, H. Berger, and E. P. F. De Lausanne, “High mobility n-type charge carriers in large single crystals,” *New York*, vol. 75, pp. 633–635, 1994.

[22] S. U. M. Khan, M. Al-Shahry, and W. B. Ingler, “Efficient photochemical water splitting by a chemically modified n-TiO_2.,” *Science (80-.).*, vol. 297, no. 5590, pp. 2243–2245, 2002.

[23] M. K. Nowotny, P. Bogdanoff, T. Dittrich, S. Fiechter, a. Fujishima, and H. Tributsch, “Observations of p-type semiconductivity in titanium dioxide at room temperature,” *Mater. Lett.*, vol. 64, no. 8, pp. 928–930, 2010.

[24] I. Lukačević, S. K. Gupta, P. K. Jha, and D. Kirin, “Lattice dynamics and Raman spectrum of rutile TiO2: The role of soft phonon modes in pressure induced phase transition,” *Mater. Chem. Phys.*, vol. 137, no. 1, pp. 282–289, 2012.

[25] K. M. Glassford and J. R. Chelikowsky, “Structural and Electronic-Properties of Titanium-Dioxide,” *Physical Review B*, vol. 46, no. 3. pp. 1284–1298, 1992.

[26] T.-D. Nguyen Phan, H.-D. Pham, T. Viet Cuong, E. Jung Kim, S. Kim, and E. Woo Shin, “A simple hydrothermal preparation of TiO_2 nanomaterials using concentrated hydrochloric acid,” *J. Cryst. Growth*, vol. 312, no. 1, pp. 79–85, Dec. 2009.

[27] H. Yang, S. Zhu, and N. Pan, “Studying the mechanisms of titanium dioxide as ultraviolet-blocking additive for films and fabrics by an improved scheme,” *J. Appl. Polym. Sci.*, vol. 92, no. 5, pp. 3201–3210, 2004.

[28] Y. Li, X. Lv, and J. Li, “High performance binderless TiO_2 nanowire arrays electrode for lithium-ion battery,” *Appl. Phys. Lett.*, vol. 95, no. 11, pp. 2009–2011, 2009.

[29] X. D. Tang, M. Chen, M. A. Joiner, N. Brot, H. Weissbach, S. H. Heinemann, J. Lykkesfeldt, C. M. Wehr, R. T. Ingersoll, J. C. Bartholomew, B. N. Ames, A. G. Pletnev, R. Putnak, and J. Speicher, “Study of Nd^{3+},Pd^{2+},Pt^{4+}, and Fe^{3+} dopant effect on photoreactivity of TiO2 nanoparticles,” *J. Biochem.*, vol. 99, no. 10, 2002.

[30] K. Byrappa and M. Yoshimura, *Handbook of Hydrothermal Technology*, 2001st ed. New York: William Andrew Publishing, 2001.

[31] R. Cherrington, D. J. Hughes, S. Senthilarasu, and V. Goodship, “Inkjet-Printed TiO_2 Nanoparticles from Aqueous Solutions for Dye-Sensitized Solar Cells (DSSCs),” *Energy Technol.*, vol. 3, no. 8, pp. 866–870, 2015.

[32] R. Govindaraj, S. M. Pandian, P. Ramasamy, and S. Mukhopadhyay, “Sol-gel synthesized mesoporous anatase titanium dioxide nanoparticles for dye sensitized solar cell (DSSC) applications,” *Bull. Mater. Sci.*, vol. 38, no. 2, pp. 291–296, 2015.

[33] S. K. Prakash, H. Singh, H. Panjiar, S. Manhas, and B. S. S. Daniel, “Application of Graphene Oxide and TiO_2 in the fabrication of Dye sensitized solar cells module by electrode modification,” *Adv. Mater. Process. Challenges Oppor.*, vol. 585, pp. 255–259, 2012.

[34] X. Chen and S. S. Mao, “Titanium Dioxide Nanomaterials : Synthesis , Properties , Modifications , and Applications,” *Chem. Rev.*, vol. 107, pp. 2891–2959, 2007.

[35] G. Peng, Y. Zhou, Y. He, X. Yu, X. a Zhang, G. Y. Li, and H. Haick, “UV-induced SiC nanowire sensors,” *J. Phys. D. Appl. Phys.*, vol. 48, no. 5, p. 55102, 2015.

[36] Z. Jakšić, M. Maksimović, and M. Sarajlić, “Silver–silica transparent metal structures as bandpass filters for the ultraviolet range,” *J. Opt. A Pure Appl. Opt.*, vol. 7, no. 1, pp. 51–55, 2004.

[37] Y. C. Lee, Z. Hassan, F. K. Yam, M. J. Abdullah, K. Ibrahim, M. Barmawi, Sugianto, M. Budiman, and P. Arifin, "A comparative study of the electrical characteristics of metal-semiconductor-metal (MSM) photodiodes based on GaN grown on silicon," *Appl. Surf. Sci.*, vol. 249, no. 1–4, pp. 91–96, 2005.

[38] M. K. Ahmad, S. M. Mokhtar, C. F. Soon, N. Nafarizal, A. B. Suriani, A. Mohamed, M. H. Mamat, M. F. Malek, M. Shimomura, and K. Murakami, "Raman investigation of rutile-phased TiO_2 nanorods/nanoflowers with various reaction times using one step hydrothermal method," *J. Mater. Sci. Mater. Electron.*, vol. 27, no. 8, pp. 7920–7926, 2016.

[39] S. Y. Lee and S. J. Park, "TiO_2 photocatalyst for water treatment applications," *J. Ind. Eng. Chem.*, vol. 19, no. 6, pp. 1761–1769, 2013.

[40] F. Suzuki, S. Fukushima, and T. Mitsui, "Application of lower titanium oxide in cosmetics," *J. Soc. Cosmet. Chem.*, vol. 64, no. February, pp. 59–64, 1978.

[41] M. J. A. Ruszala, N. A. Rowson, L. M. Grover, and R. A. Choudhery, "Low Carbon Footprint TiO_2 Substitutes in Paint: A Review," *Int. J. Chem. Eng. Appl.*, vol. 6, no. 5, pp. 331–340, 2015.

[42] S. El-Sherbiny, F. Morsy, M. Samir, and O. a. Fouad, "Synthesis, characterization and application of TiO_2 nanopowders as special paper coating pigment," *Appl. Nanosci.*, vol. 4, no. 3, pp. 305–313, 2013.

[43] P. Soundarrajan, K. Sankarasubramanian, T. Logu, K. Sethuraman, and K. Ramamurthi, "Growth of rutile TiO_2 nanorods on TiO_2 seed layer prepared using facile low cost chemical methods," *Mater. Lett.*, vol. 116, pp. 191–194, Feb. 2014.

[44] C. Cao, C. Hu, X. Wang, S. Wang, Y. Tian, and H. Zhang, "UV sensor based on TiO_2 nanorod arrays on FTO thin film," *Sensors Actuators, B Chem.*, vol. 156, no. 1, pp. 114–119, Aug. 2011.

[45] C. Wang, Z. Jiang, L. Wei, Y. Chen, J. Jiao, M. Eastman, and H. Liu, "Photosensitization of TiO_2 nanorods with CdS quantum dots for photovoltaic applications : A wet-chemical approach," *Nano Energy*, vol. 1, no. 3, pp. 440–447, 2012.

[46] Y. X. Zhang, G. H. Li, Y. X. Jin, Y. Zhang, J. Zhang, and L. D. Zhang, "Hydrothermal synthesis and photoluminescence of TiO_2 nanowires," vol. 365, pp. 300–304, 2002.

[47] V. Manthina, J. Pablo, C. Baena, G. Liu, and A. G. Agrios, "ZnO − TiO_2 Nanocomposite Films for High Light Harvesting E ffi ciency and Fast Electron Transport in Dye-Sensitized Solar Cells," 2012.

[48] Z. Liu, X. Su, G. Hou, S. Bi, Z. Xiao, and H. Jia, "Spherical TiO_2 aggregates with different building units for dye-sensitized solar cells.," *Nanoscale*, vol. 5, no. 17, pp. 8177–83, 2013.

[49] W. Guo, C. Xu, X. Wang, S. Wang, C. Pan, C. Lin, and Z. L. Wang, "Rectangular bunched rutile TiO_2 nanorod arrays grown on carbon fiber for dye-sensitized solar cells.," *J. Am. Chem. Soc.*, vol. 134, no. 9, pp. 4437–41,

2012.

[50] H. Zhang, P. Liu, X. Liu, S. Zhang, X. Yao, T. An, R. Amal, and H. Zhao, "Fabrication of highly ordered TiO_2 nanorod/nanotube adjacent arrays for photoelectrochemical applications," *Langmuir*, vol. 26, no. 13, pp. 11226–11232, 2010.

[51] B. Koo, J. Park, Y. Kim, S. H. Choi, Y. E. Sung, and T. Hyeon, "Simultaneous phase- and size-controlled synthesis of TiO_2 nanorods via non-hydrolytic sol-gel reaction of syringe pump delivered precursors," *J. Phys. Chem. B*, vol. 110, no. 48, pp. 24318–24323, 2006.

[52] S. J. Limmer, T. P. Chou, and G. Z. Cao, "A study on the growth of TiO_2 nanorods using sol electrophoresis," *J. Mater. Sci. Mater. Electron.*, vol. 9, no. 39, pp. 895–901, 2004.

[53] K. Fujihara, A. Kumar, R. Jose, S. Ramakrishna, and S. Uchida, "Spray deposition of electrospun TiO_2 nanorods for dye-sensitized solar cell," *Nanotechnology*, vol. 18, no. 365709, pp. 1–6, 2007.

[54] G. R. A. Kumara, M. Okuya, K. Murakami, S. Kaneko, V. V. Jayaweera, and K. Tennakone, "Dye-sensitized solid-state solar cells made from magnesiumoxide-coated nanocrystalline titanium dioxide films: Enhancement of the efficiency," *J. Photochem. Photobiol. A Chem.*, vol. 164, no. 1–3, pp. 183–185, 2004.

[55] S. Yang, L. Gao, and S. Microstructure, "Fabrication and Characterization of Nanostructurally Flowerlike Aggregates of TiO_2 via a Surfactant-free Solution Route : Effect of Various Reaction Media," vol. 34, no. 7, pp. 1044–1045, 2005.

[56] S. Yang, L. Gao, and S. Microstructure, "Low-temperature Synthesis of Crystalline TiO_2 Nanorods : Mass Production Assisted by Surfactant," vol. 34, no. 7, pp. 964–965, 2005.

[57] J. J. Yuan, H. D. Li, S. Y. Gao, D. D. Sang, L. a. Li, and D. Lu, "Hydrothermal synthesis, characterization and properties of TiO_2 nanorods on boron-doped diamond film," *Mater. Lett.*, vol. 64, no. 18, pp. 2012–2015, 2010.

[58] X. Ji, W. Liu, Y. Leng, and A. Wang, "Facile Synthesis of ZnO@TiO_2 Core-Shell Nanorod Thin Films for Dye-Sensitized Solar Cells," *J. Nanomater.*, vol. 2015, pp. 1–5, 2015.

[59] Y. Wang, L. Zhang, K. Deng, X. Chen, and Z. Zou, "Low Temperature Synthesis and Photocatalytic Activity of Rutile TiO_2 Nanorod Superstructures," *J. Phys. Chem. C*, vol. 111, pp. 2709–2714, 2007.

[60] M. N. Tahir, M. N. Tahir, P. Theato, P. Theato, P. Oberle, P. Oberle, G. Melnyk, G. Melnyk, S. Faiss, S. Faiss, U. Kolb, U. Kolb, A. Janshoff, A. Janshoff, M. Stepputat, M. Stepputat, W. Tremel, and W. Tremel, "Facile Synthesis and Characterization of Functionalized, Monocrystalline Rutile TiO $_2$ Nanorods," *Am. Chem. Soc.*, no. 21, pp. 5209–5212, 2006.

[61] Y. Li, M. Guo, M. Zhang, and X. Wang, “Hydrothermal synthesis and characterization of TiO_2 nanorod arrays on glass substrates,” *Mater. Res. Bull.*, vol. 44, no. 6, pp. 1232–1237, 2009.

[62] L. Dong, K. Cheng, W. Weng, C. Song, P. Du, G. Shen, and G. Han, “Hydrothermal growth of rutile TiO_2 nanorod films on titanium substrates,” *Thin Solid Films*, vol. 519, no. 15, pp. 4634–4640, 2011.

[63] H.-E. Wang, Z. Chen, Y. H. Leung, C. Luan, C. Liu, Y. Tang, C. Yan, W. Zhang, J. A. Zapien, I. Bello, and S.-T. Lee, “Hydrothermal synthesis of ordered single-crystalline rutile TiO_2 nanorod arrays on different substrates,” *Appl. Phys. Lett.*, vol. 96, no. 26, p. 263104, 2010.

[64] S. Venkatachalam, H. Hayashi, T. Ebina, and H. Nanjo, “Preparation and Characterization of Nanostructured TiO_2 Thin Films by Hydrothermal and Anodization Methods,” 2013.

[65] S. P. Chang, R. W. Chuang, S. J. Chang, C. Y. Lu, Y. Z. Chiou, and S. F. Hsieh, “Surface HCl treatment in ZnO photoconductive sensors,” *Thin Solid Films*, vol. 517, no. 17, pp. 5050–5053, 2009.

[66] D. Caputo, G. de Cesare, a. Nascetti, and M. Tucci, “Innovative window layer for amorphous silicon/amorphous silicon carbide UV sensor,” *J. Non. Cryst. Solids*, vol. 352, no. 9–20 SPEC. ISS., pp. 1818–1821, 2006.

[67] J. D. Hwang and C. C. Lin, “Gallium nitride photoconductive ultraviolet sensor with a sputtered transparent indium-tin-oxide ohmic contact,” *Thin Solid Films*, vol. 491, no. 1–2, pp. 276–279, 2005.

[68] K. Hayashi, Y. Yokota, T. Tachibana, K. Kobashil, J. Achard, A. Gicquel, C. Olivero, M. C. Castex, and A. Treshchalov, “Temporal response of UV sensors made of highly oriented diamond films by 193 and 313 nm laser pulses,” *Diam. Relat. Mater.*, vol. 10, no. 9–10, pp. 1794–1798, 2001.

[69] G. Y. Chen and Z. Wang, “Towards Extremely Sensitive Ultraviolet-Light Sensors Employing Photochromic Optical Microfiber,” *J. sensors*, vol. 2015, pp. 1–7, 2015.

[70] D. C. Look, “Recent advances in ZnO materials and devices,” *Mater. Sci. Eng. B Solid-State Mater. Adv. Technol.*, vol. 80, no. 1–3, pp. 383–387, 2001.

[71] H. Jeong, K. S. Kim, Y. H. Kim, H. Jeong, H. Song, K. H. Lee, M. S. Jeong, D. Wang, and G. Y. Jung, “A crossbar-type high sensitivity ultraviolet photodetector array based on a one hole-one nanorod configuration via nanoimprint lithography.,” *Nanotechnology*, vol. 22, no. 27, p. 275310, 2011.

[72] X. Zu, H. Wang, G. Yi, Z. Zhang, X. Jiang, J. Gong, and H. Luo, “Self-powered UV photodetector based on heterostructured TiO_2 nanowire arrays and polyaniline nanoflower arrays,” *Synth. Met.*, vol. 200, pp. 58–65, 2015.

[73] H. Wang, G. Yi, X. Zu, X. Jiang, Z. Zhang, and H. Luo, “A highly sensitive and self-powered ultraviolet photodetector composed of titanium dioxide nanorods and polyaniline nanowires,” *Mater. Lett.*, vol. 138, pp. 204–207, 2015.

[74] W. F. Xiang, P. R. Yang, a. J. Wang, K. Zhao, H. Ni, and S. X. Zhong, "Vertical geometry ultraviolet photodetectors with high photosensitivity based on nanocrystalline TiO_2 films," *Thin Solid Films*, vol. 520, no. 24, pp. 7144–7146, 2012.

[75] M. Okuya, K. Shiozaki, N. Horikawa, T. Kosugi, G. R. A. Kumara, J. Á. Madarász, S. Kaneko, and G. Pokol, "Porous TiO_2 thin films prepared by spray pyrolysis deposition (SPD) technique and their application to UV sensors," *Solid State Ionics*, vol. 172, no. 1–4 SPEC. ISS., pp. 527–531, 2004.

[76] A. M. Selman and Z. Hassan, "Highly sensitive fast-response UV photodiode fabricated from rutile TiO_2 nanorod array on silicon substrate," *Sensors Actuators A Phys.*, vol. 221, pp. 15–21, Jan. 2015.

[77] M. H. Mamat, "Fabrication and Characterisation of Aligned Zinc Oxide Nanorod Array-Based Ultraviolet Photoconductive Sensors," Universiti Teknologi Mara, 2013.

[78] C. Soci, a. Zhang, B. Xiang, S. a. Dayeh, D. P. R. Aplin, J. Park, X. Y. Bao, Y. H. Lo, and D. Wang, "ZnO nanowire UV photodetectors with high internal gain," *Nano Lett.*, vol. 7, no. 4, pp. 1003–1009, 2007.

[79] S. A. Yousaf and S. Ali, "The Effect of Fluorine Doping on Optoelectronic Properties of Tin-Dioxide Thin Films," *Pak. J. Sci. Ind. Res.*, vol. 48, no. 1 & 2, pp. 43–50, 2009.

[80] G. Wu, J. Wang, D. F. Thomas, and A. Chen, "Synthesis of F-doped flower-like TiO_2 nanostructures with high photoelectrochemical activity," *Langmuir*, vol. 24, no. 7, pp. 3503–3509, 2008.

[81] M. Li, Y. Jiang, R. Ding, D. Song, H. Yu, and Z. Chen, "Hydrothermal synthesis of anatase TiO_2 nanoflowers on a nanobelt framework for photocatalytic applications," *J. Electron. Mater.*, vol. 42, no. 6, pp. 1290–1296, 2013.

[82] P. Dong, Y. Wang, B. Liu, L. Guo, Y. Huang, and S. Yin, "Effect of hydrothermal reaction time on morphology and photocatalytic activity of $H_2Ti_3O_7$ nanotubes obtained via a rapid synthesis route," *Appl. Surf. Sci.*, vol. 258, no. 18, pp. 7052–7058, 2012.

[83] B. Grzmil, B. Kic, and M. Rabe, "Inhibition of the Anatase — Rutile Phase Transformation with," *Chem.Pap.*, vol. 58, no. May, pp. 410–414, 2004.

[84] H. H. Nguyen, D.-J. Kim, D.-W. Park, and K.-S. Kim, "Effect of initial precursor concentration on TiO_2 thin film nanostructures prepared by PCVD system," *J. Energy Chem.*, vol. 22, no. 3, pp. 375–381, May 2013.

[85] B. Liu and E. S. Aydil, "Growth of Oriented Single-Crystalline Rutile TiO Nanorods on Transparent Conducting Substrates for Dye-Sensitized Solar Cells Growth of Oriented Single-Crystalline Rutile TiO_2 Nanorods on Transparent Conducting Substrates for Dye-Sensitized Solar Cells," *Glass*, no. 9, pp. 3985–3990, 2009.

[86] S. Cells, “Hydrothermal Fabrication of Hierarchically Anatase TiO_2 Nanowire,” *Sci. Rep.*, vol. 3, no. 1352, pp. 1–7, 2013.

[87] P. Soundarrajan, K. Sankarasubramanian, K. Sethuraman, and K. Ramamurthi, “by facile low cost chemical methods,” *CrystEngComm*, pp. 8756–8768, 2014.

[88] X. Xue, W. Ji, Z. Mao, H. Mao, Y. Wang, X. Wang, W. Ruan, B. Zhao, and J. R. Lombardi, “Raman Investigation of Nanosized TiO_2 : Effect of Crystallite Size and Quantum Confinement.” 2012.

[89] B. Journal, G. C. Collazzo, S. L. Jahn, and E. L. Foletto, “Temperature And Reaction Time Effects On The Structural Properties Of Titanium Dioxide Nanopowders Obtained Via The Hydrothermal Method,” vol. 28, no. 2, pp. 265–272, 2011.

[90] L. D. Atsov, C. Kormann, and W. Plietht, “Electrochemical Synthesis and In Situ Raman Spectroscopy of Thin Films of Titanium Dioxide,” vol. 22, no. May, pp. 573–575, 1991.

[91] H. L. Ma, J. Y. Yang, Y. Dai, Y. B. Zhang, B. Lu, and G. H. Ma, “Raman study of phase transformation of TiO_2 rutile single crystal irradiated by infrared femtosecond laser,” *Appl. Surf. Sci.*, vol. 253, no. 18, pp. 7497–7500, 2007.

[92] H. W. Kim, H. S. Kim, H. G. Na, J. C. Yang, and D. Y. Kim, “Growth, structural, Raman, and photoluminescence properties of rutile TiO_2 nanowires synthesized by the simple thermal treatment,” *J. Alloys Compd.*, vol. 504, no. 1, pp. 217–223, Aug. 2010.

[93] P. Dong, Y. Wang, B. Liu, L. Guo, Y. Huang, and S. Yin, “Applied Surface Science Effect of hydrothermal reaction time on morphology and photocatalytic activity of $H_2Ti_3O_7$ nanotubes obtained via a rapid synthesis route,” *Appl. Surf. Sci.*, vol. 258, no. 18, pp. 7052–7058, 2012.

[94] H. Chen, C. Su, J. Chen, T. Yang, N. Hsu, and W. Li, “Preparation and Characterization of Pure Rutile TiO_2 Nanoparticles for Photocatalytic Study and Thin Films for Dye-Sensitized Solar Cells,” vol. 2011, 2011.

[95] J. G. and L. T. Qiuxiang Wen, Jun Yu, Xiaoyong Sun, Jia Zhuang*, Quangui He, Xin You, “Hydrothermal Treatment TiO_2 Film by Hydrochloric Acid for Efficient Dye- sensitized Solar Cells,” *R. Soc. Chem.*, vol. 1, no. 1, pp. 1–6, 2016.

[96] P. Isi and P. Asid, “Influence of Hydrochloric Acid Volume on the Growth of Titanium Dioxide (TiO_2) Nanostructures by Hydrothermal Method,” vol. 45, no. 11, pp. 1669–1673, 2016.

[97] J. Lind, “Effect of synthesis duration and HCl acid concentration on the formation of hydrothermally synthesised TiO_2 nanoparticles by,” Cape Peninsula University of Technology, 2015.

[98] Z. Tan, K. Sato, and S. Ohara, “Synthesis of layered nanostructured TiO_2 by hydrothermal method,” *Adv. Powder Technol.*, no. 26, pp. 296–302, Nov. 2014.

[99] J. Kim, K. Lee, J. Roh, S. Song, J. Park, I. Yer, and B. Moon, “Ga-doped ZnO transparent electrodes with TiO_2 blocking layer / nanoparticles for dye-sensitized solar cells,” pp. 2–5, 2012.

[100] J. J. Zhou, S. Y. Wang, and S. Gunasekaran, “Preparation and characterization of whey protein film incorporated with TiO_2 nanoparticles,” *J. Food Sci.*, vol. 74, no. 7, pp. 50–56, 2009.

[101] S. K. Kuriechen, S. Murugesan, and S. P. Raj, “Mineralization of Azo Dye Using Combined Photo-Fenton and Photocatalytic Processes under Visible Light,” *J. Catal.*, vol. 2013, pp. 1–6, 2013.

[102] G. Yang, Z. Jiang, H. Shi, T. Xiao, and Z. Yan, “Preparation of highly visible-light active N-doped TiO_2 photocatalyst,” *J. Mater. Chem.*, vol. 20, no. 25, pp. 5301–5309, 2010.

[103] J. Tian, Y. Sang, Z. Zhao, W. Zhou, D. Wang, X. Kang, H. Liu, J. Wang, S. Chen, H. Cai, and H. Huang, “Enhanced photocatalytic performances of CeO_2/TiO_2 nanobelt heterostructures,” *Small*, vol. 9, no. 22, pp. 3864–3872, 2013.

[104] R. van de Krol and Michael Grätzel, *Principles of Photoelectrochemical Cells*, vol. 102. Springer US, 2012.

[105] A. J. Bard, “Design of Semiconductor Photoelectrochemical Systems for Solar Energy Conversion,” *J. Phys. Chem. C*, vol. 86, no. May, pp. 172–177, 1982.

[106] H. Li, L. Zheng, S. Shu, H. Cheng, and Y. Yang, “Morphology Control of Anodic TiO_2 Nanomaterials via Cold Work Pretreatment of Ti Foils,” *J. Electrochem. Soc.*, vol. 158, no. 10, pp. 346–351, 2011.

[107] A. M. Selman and Z. Hassan, “Effects of variations in precursor concentration on the growth of rutile TiO_2 nanorods on Si substrate with fabricated fast-response metal–semiconductor–metal UV detector,” *Opt. Mater. (Amst).*, vol. 44, pp. 37–47, Jun. 2015.

[108] Y. Xie, L. Wei, G. Wei, Q. Li, D. Wang, Y. Chen, S. Yan, G. Liu, L. Mei, and J. Jiao, “A self-powered UV photodetector based on TiO_2 nanorod arrays,” *Nanoscale Res. Lett.*, vol. 8, no. 188, pp. 1–6, 2013.

[109] C. Cao, C. Hu, W. Shen, S. Wang, S. Song, and M. Wang, “Improving photoelectrochemical performance by building Fe_2O_3 heterostructure on TiO_2 nanorod arrays,” *Mater. Res. Bull.*, vol. 70, no. 3, pp. 155–162, 2015.